Journal of ELECTRONIC MATERIALS, Vol. 39, No. 9, 2010
DOI: 10.1007/s11664-010-1232-2

Improved Thermoelectric Properties of Bi-M-Co-O (M = Sr, Ca) Misfit Compounds by Laser Directional Solidification

J.C. DIEZ,[1] SH. RASEKH,[1] M.A. MADRE,[1] E. GUILMEAU,[2] S. MARINEL,[2] and A. SOTELO[1,3]

1.—Instituto de Ciencia de Materiales de Aragón (ICMA), CSIC-Universidad de Zaragoza, C/Mª de Luna 3, 50018 Zaragoza, Spain. 2.—Laboratoire CRISMAT, UMR 6508 CNRS-ENSICAEN, 6 Boulevard du Maréchal Juin, 14050 Caen Cedex, France. 3.—e-mail: asotelo@unizar.es

In this work, improvement of the thermoelectric properties of bulk samples due to texture developed by a directional laser-assisted solidification process (laser floating zone melting method) is reported for cobaltite materials with compositions $Bi_2Sr_2Co_{1.8}O_y$ and $Bi_2Ca_2Co_{1.7}O_y$. Sample composition and microstructure have been studied using x-ray diffraction and scanning electron microscopy. Thermoelectric properties have been measured between 4 K and 300 K by simultaneous determination of electrical resistivity and thermopower. All textured samples showed remarkable increase of power factor values as compared with conventional sintered ceramics.

Key words: Thermoelectric oxides, misfit cobaltites, thermoelectric properties, directional solidification, laser floating zone

INTRODUCTION

In response to the escalating energy crisis and related pollution problems, we urgently need to adopt new technologies that utilize energy sources in a more efficient and ecological manner. Thermoelectric power generation has been recognized as one of the innovative and promising energy conservation and environmentally friendly technologies.[1] It enables conversion of a thermal gradient originating, for example, from exhaust emissions, into an electrical energy output by the well-known Seebeck effect. Among other advantages, thermoelectric generation is reliable, clean, and silent. On the other hand, large efforts are still required to obtain more efficient thermoelectric materials and devices.

Since the discovery of large room-temperature thermopower (TEP) in $NaCo_2O_4$,[2] other layered cobalt oxides, such as Ca-Co-O,[3] Bi-Ca-Co-O,[4] and Bi-Sr-Co-O,[5] have attracted much attention. Their crystal structure is composed of alternate stacking of a common conductive CdI_2-type CoO_2 layer with a two-dimensional triangular lattice and a block layer, composed of insulating rock-salt-type layers.[4,6,7] This structure shows high crystal anisotropy, which is reflected in their thermoelectric properties and preferential grain growth along the *ab*-planes, which are also the conductive ones.

The performance of thermoelectric materials is evaluated through a dimensionless parameter known as the figure of merit ($ZT = S^2T/\rho\kappa$), where S is the TEP, T is the absolute temperature, ρ is the electrical resistivity, and κ is the thermal conductivity. An easy way to increase this figure of merit is through the use of materials with high working temperature. This can be achieved using thermoelectric ceramics, which possess the advantages of higher thermal stability at high temperature and lower toxicity as compared with conventional semiconducting compounds and alloys. In this context, those cobalt oxides seem to be alternatives for thermoelectric power generation devices.

Another way to increase ZT is through improvement of grain orientation using various texturing techniques. Some of these involve solid-state reactions, such as hot forging[8] and template grain growth.[9] On the other hand, it is also possible to

(Received June 26, 2009; accepted April 7, 2010; published online May 29, 2010)

obtain well-oriented grains by directional solidification from molten material, as in the laser floating zone (LFZ) process.[10]

Herein, we report the main microstructural and thermoelectric results obtained on bulk textured $Bi_2Sr_2Co_{1.8}O_y$ and $Bi_2Ca_2Co_{1.7}O_y$ misfit cobaltites obtained by a laser-assisted directional solidification process.

EXPERIMENTAL PROCEDURES

$Bi_2Ca_2Co_{1.7}O_y$ and $Bi_2Sr_2Co_{1.8}O_y$ polycrystalline samples were prepared by a conventional solid-state route using commercial Bi_2O_3 (Panreac, 98+%), $CaCO_3$ (Panreac, 98+%), $SrCO_3$ (Panreac, 98+%), and Co_2O_3 (Aldrich, 98+%) powders as starting materials. They were weighed in appropriate proportions, mixed, and ball-milled for 30 min at 300 rpm in agate medium. In order to ensure complete decomposition of the carbonates, mixed powders were thermally treated twice, at 750°C and 800°C, for 12 h under air, with manual milling in between. This thermal treatment is of great importance, as it has been designed to decompose the calcium and strontium carbonates. This treatment avoids the presence of carbonates in the LFZ process, as they would decompose in the melting process, forming bubbles inside the liquid and, more important, disturbing the crystallization front. The so-obtained powders were then isostatically pressed at 200 MPa for 1 min to obtain green cylindrical ceramic bars, which were subsequently used as feed in a LFZ device equipped with a continuous power Nd:YAG solid-state laser (1.06 μm), as described elsewhere.[11]

The texturing processes were performed downwards with a growth speed of 30 mm/h. The feed was rotated at 15 rpm to ensure compositional homogeneity of the molten zone and to maintain constant textured rod diameter. The use of this relatively high crystallization rate implies that the growth process does not occur in equilibrium. For this reason, the obtained textured cylinders are formed by the most stable phase, but accompanied by other phases (secondary phases). In spite of this multiphasic composition, the LFZ process allows the production of long (more than 20 cm) textured cylinders with ~2 mm diameter. These bars were finally cut to obtain samples having adequate dimensions for characterization.

Powder x-ray diffraction (XRD) patterns were systematically recorded by using a Siemens Kristalloflex diffractometer working with Cu K_α radiation and 2θ ranging between 10° and 40° in order to identify the different phases in the thermoelectric textured materials.

Microstructures were observed by using a JEOL 6000 scanning electron microscope (SEM) equipped with an energy-dispersive spectroscopy (EDS) device used for phase identification. On the one hand, micrographs of longitudinal fractured sections were recorded to observe grain orientation. Longitudinal and transversal polished sections of the samples were also observed to analyze the composition and distribution of the different phases.

Electrical resistivity measurements were performed following the growth axis on textured cylinders using the standard direct-current (DC) four-probe technique at temperatures between 5 K and 400 K using a physical properties measurement system from Quantum Design. TEP was determined at temperatures between 5 K and 300 K using an experimental setup that has been described elsewhere.[12] To determine the thermoelectric performance of the samples, the power factor (PF = S^2/ρ) was calculated from electrical resistivity and TEP data.

RESULTS AND DISCUSSION

Powder XRD patterns confirmed that the cobaltite phase is the major one, independent of the composition. These patterns show very intense peaks for the (002l) planes, indicating that the cobaltite grains grow preferentially along the *ab*-plane. This growth habit is clearly confirmed in the micrograph displayed in Fig. 1, which shows a representative fractured longitudinal section of a textured sample. In this figure, it can be clearly seen that grain lengths exceed 100 μm along the *ab*-plane.

Polished longitudinal surfaces of the two textured bars with different compositions are shown in Fig. 2. At first sight, it is clear that $Bi_2Sr_2Co_{1.8}O_y$ (Fig. 2b) is formed by larger and better oriented grains than is $Bi_2Ca_2Co_{1.7}O_y$ (Fig. 2a). More detailed analysis of this figure reveals further differences between them. In Fig. 2a, it is possible to distinguish three different contrasts: black contrast with a relatively small size compared with the other

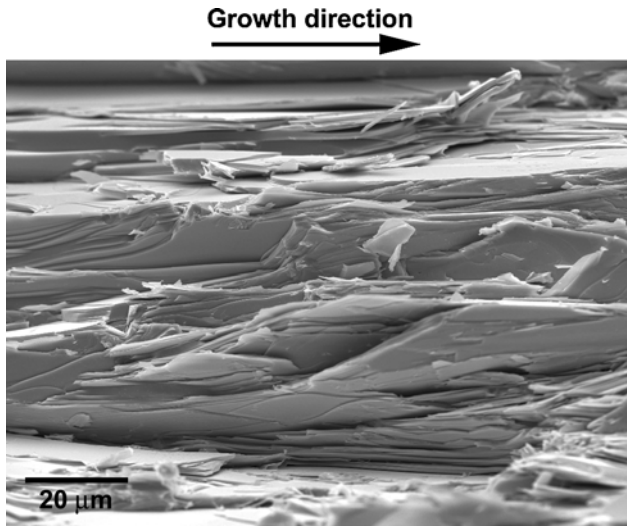

Fig. 1. SEM micrograph of a longitudinal fractured sample ($Bi_2Sr_2Co_{1.8}O_y$), showing the typical orientation of the misfit plate-like grains. The arrow indicates the growth direction.

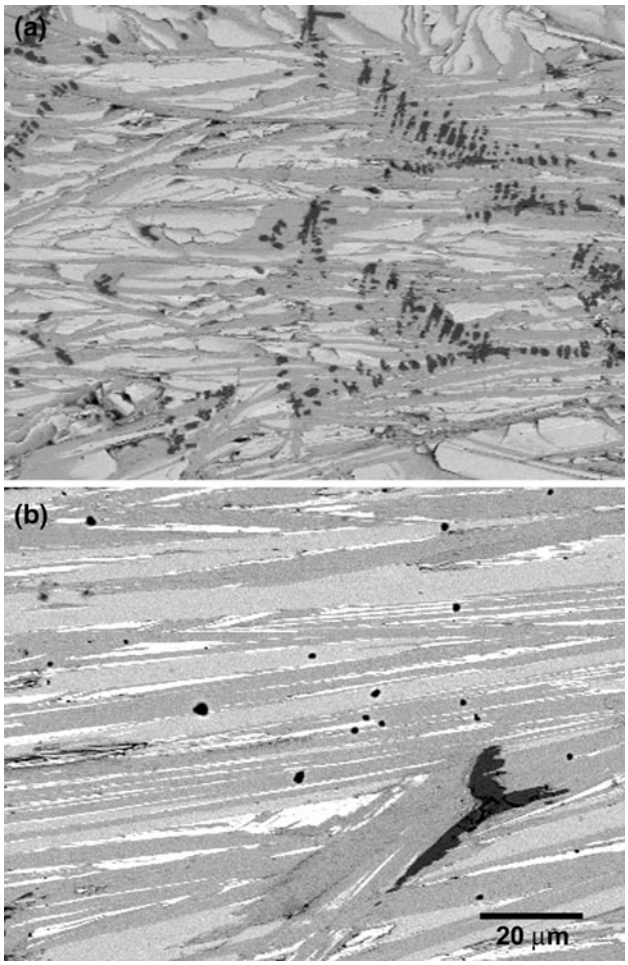

Fig. 2. SEM micrographs of longitudinal polished sections of textured samples of: (a) $Bi_2Ca_2Co_{1.7}O_y$ and (b) $Bi_2Sr_2Co_{1.8}O_y$.

phases, showing a dendritic-like structure and identified as CoO on EDS analysis; dark grey contrast, which has been associated with $Bi_2Ca_2Co_2O_y$ cobaltite; and light grey contrast, which is a non-thermoelectric phase corresponding to Bi-Ca-O solid solution. Both gray contrasts appear as alternate layers with preferential orientation along the growth direction. On the other hand, four different contrasts can be observed in Fig. 2b: black corresponding to CoO, and white, identified as nonthermoelectric Bi-Sr-O solid solution; in addition to these secondary phases, the samples are mainly composed of alternately stacked dark and light gray contrasts corresponding to thermoelectric $Bi_2Sr_2Co_2O_y$ and $Bi_2Sr_2Co_{1.3}O_y$ phases, respectively. Moreover, the relative proportion of secondary phases is also reduced from the Ca-containing samples (about 35%) to the Sr-containing ones (about 10%), measured as the relative areas of the different phases obtained from SEM micrographs.

The temperature dependence of the electrical resistivity of the textured materials is shown in Fig. 3 for both compositions. As can be easily seen, the two $\rho(T)$ curves exhibit semiconductor-like

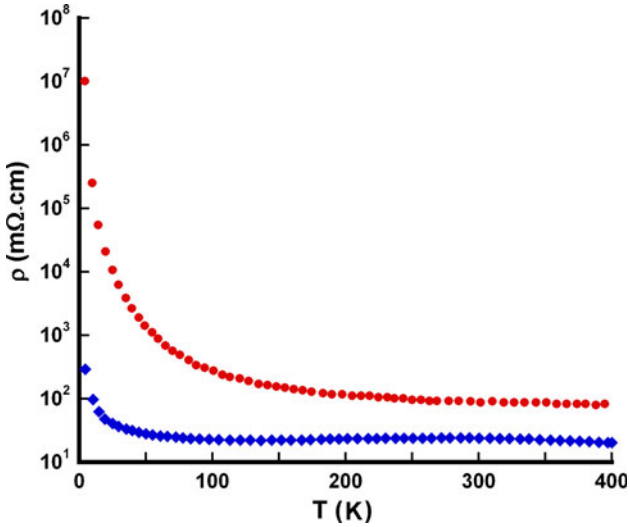

Fig. 3. Temperature dependence of ρ for the different compositions: (●) $Bi_2Ca_2Co_{1.7}O_y$ and (◆) $Bi_2Sr_2Co_{1.8}O_y$.

behavior from low to high temperature, characterized by $d\rho/dT < 0$. This semiconducting behavior is in agreement with earlier reports on these cobaltite systems.[7,13] The resistivity values decrease from the Ca-containing samples (about 91 mΩ cm at room temperature) to the Sr-containing ones (about 24 mΩ cm at room temperature). The obtained values are very similar to those reported in the literature for these types of materials. The apparently contradictory results measured in these highly textured materials can be associated with the presence of secondary phases (usually not present in adequately sintered materials) and a reduction of the oxygen content in comparison with sintered specimens. In both cases the samples show three-dimensional Mott variable-range hopping (VRH), with $\ln \rho \propto T^{-1/4}$ over a wide temperature range. More detailed observation of this graph shows slight deviation from semiconductor behavior between 150 K and 250 K for the Sr-containing samples. In this temperature range, a change of sign of $d\rho/dT$ is produced, indicating more metallic-like behavior, which is in agreement with previously reported data.[14,15]

Figure 4 shows the temperature dependence of the TEP as a function of nominal composition. The sign of the TEP is positive over the entire measured temperature range, confirming a mechanism involving hole conduction. In both cases, TEP values increase with temperature until about 150 K, showing good agreement with $S \propto T^{1/2}$, which is also described by the three-dimensional Mott VRH conduction mechanism. From 150 K to room temperature, the TEP is practically constant, as has been previously reported for thermoelectric cobaltites.[16] At room temperature, TEP values are about 205 μV/K for the Ca-containing samples and 130 μV/K for the Sr-containing samples ones. These values are

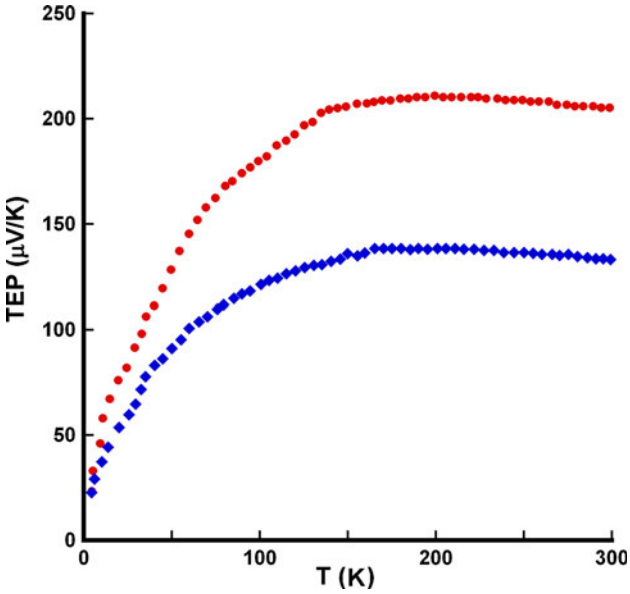

Fig. 4. Temperature dependence of TEP for the different compositions: (●) $Bi_2Ca_2Co_{1.7}O_y$ and (◆) $Bi_2Sr_2Co_{1.8}O_y$.

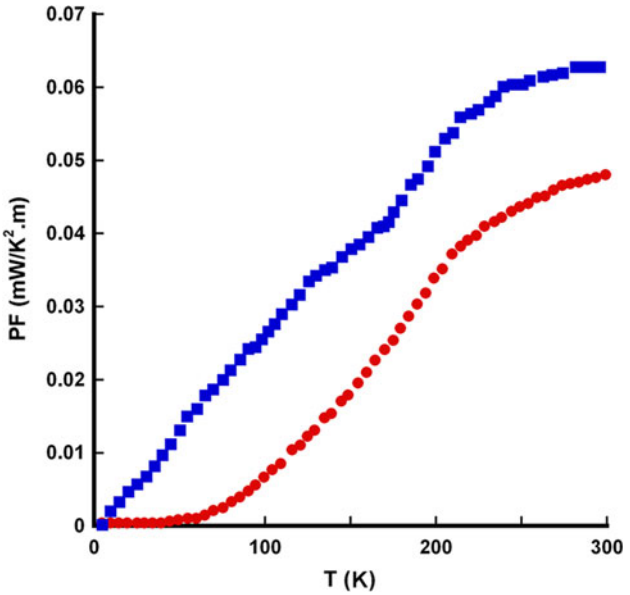

Fig. 5. Temperature dependence of PF for the different compositions: (●) $Bi_2Ca_2Co_{1.7}O_y$ and (◆) $Bi_2Sr_2Co_{1.8}O_y$.

higher than those reported in the literature[6] and are not common in these systems, but we can assume that the LFZ growth can probably generate oxygen vacancies in larger content than in bulk samples synthesized by a classic solid-state reaction. This oxygen content reduction has been confirmed by thermogravimetric measurements and estimated at about 1 wt.% to 2 wt.%. As a consequence, the hole concentration is decreased due to the reduction of Co^{4+} to Co^{3+}, resulting in increased TEP.[15] It has already been evidenced that, in reduced conditions, the misfit phase $[Ca_2CoO_3][CoO_2]_{1.62}$ is not stoichiometric in oxygen but contains considerable amounts of oxygen vacancies.[17] Moreover, the lower TEP values in the plateau-like region for Sr-containing samples, compared with the Ca-containing ones, confirms the more metallic-like behavior observed in the resistivity measurements.

Finally, in order to evaluate the thermoelectric performance of these materials, the PF was calculated. From the data represented in Figs. 3 and 4 the temperature dependence of the PF was calculated for both compositions and is shown in Fig. 5. The two different compositions showed similar behavior with temperature. The PF reached maximum values at room temperature, being about 0.05 mW/K^2m and 0.06 mW/K^2m for the $Bi_2Ca_2Co_{1.7}O_y$ and $Bi_2Sr_2Co_{1.8}O_y$ samples, respectively. In both cases these values are higher than the usual ones reported for sintered specimens.

CONCLUSIONS

Microstructural and thermoelectric characteristics of LFZ directionally grown $Bi_2Sr_2Co_{1.8}O_y$ and $Bi_2Ca_2Co_{1.7}O_y$ misfit cobaltites have been studied. The following conclusions can be drawn from this study:

1. The LFZ method has been successfully applied for growing bulk samples of misfit cobaltites, leading to highly textured samples with homogeneous dimensions and phase distribution.
2. The Sr-containing samples show larger and better oriented grains, and a lower amount of secondary phases, as compared with the Ca-containing ones.
3. TEP values at room temperature are higher than those found in sintered ceramics. On the other hand, their evolution is in agreement with data reported in the literature as a function of alkaline-earth cation size.
4. Electrical resistivity values are similar to those obtained for sintered bulk ceramics in both cases.
5. A substantial increase of the PF has been obtained as a result of increasing the TEP in $Bi_2Sr_2Co_{1.8}O_y$ and $Bi_2Ca_2Co_{1.7}O_y$ cobaltites.
6. The obtained results indicate that the LFZ process is a very useful and promising technique to obtain well-textured bulk misfit cobaltites with improved thermoelectric properties.

ACKNOWLEDGEMENTS

The authors wish to thank the Gobierno de Aragón (Project PI154/08 and Research Groups T12 and T74), the Spanish–French Integrated Action (HF2006-0171), and the Spanish Ministry of Science and Innovation (Project MAT2008-00429 and Project CEN 2007-2014) for financial support. The technical contributions of C. Estepa, J.A. Gómez, and C. Gallego are also acknowledged.

REFERENCES

1. T. Kajikawa, *J. Electron. Mater.* 38, 1083 (2009). doi:10.1007/s11664-009-0831-2.
2. I. Terasaki, Y. Sasago, and K. Uchinokura, *Phys. Rev. B* 56, R12685 (1997). doi:10.1103/PhysRevB.56.R12685.
3. S.W. Li, R. Funahashi, I. Matsubara, K. Ueno, S. Sodeoka, and H. Yamada, *J. Mater. Chem.* 9, 1659 (1999).
4. A. Maignan, S. Hébert, M. Hervieu, C. Michel, D. Pelloquin, and D. Khomskii, *J. Phys.: Condens. Matter* 15, 2711 (2003). doi:10.1088/0953-8984/15/17/323.
5. R. Funahashi, I. Matsubara, and S. Sodeoka, *Appl. Phys. Lett.* 76, 2385 (2000). doi:0003-6951/2000/76(17)/2385/3/$17.00.
6. H. Itahara, C. Xia, J. Sugiyama, and T. Tani, *J. Mater. Chem.* 14, 61 (2004). doi:10.1039/b309804d.
7. E. Guilmeau, M. Mikami, R. Funahashi, and D. Chateigner, *J. Mater. Res.* 20, 1002 (2005). doi:10.1557/JMR.2005.0131.
8. V. Garnier, R. Caillard, A. Sotelo, and G. Desgardin, *Physica C* 319, 197 (1999). doi:10.1016/S0921-4534(99)00308-1.
9. M.M. Seabaugh, I.H. Kerscht, and C.L. Messing, *J. Am. Ceram. Soc.* 80, 1181 (1997).
10. A. Sotelo, E. Guilmeau, M.A. Madre, S. Marinel, J.C. Diez, and M. Prevel, *J. Eur. Ceram. Soc.* 27, 3697 (2007). doi:10.1016/j.jeurceramsoc.2007.02.020.
11. J.C. Diez, L.A. Angurel, H. Miao, J.M. Fernandez, and G.F. de la Fuente, *Supercond. Sci. Technol.* 11, 101 (1998). doi:10.1088/0953-2048/11/1/020.
12. J. Hejtmanek, Z. Jirak, M. Marysko, C. Martin, A. Maignan, M. Hervieu, and B. Raveau, *Phys. Rev. B* 60, 14057 (1999). doi:0163-1829/99/60(20)/14057(9)/$15.00.
13. E. Guilmeau, M. Pollet, D. Grebille, D. Chateigner, B. Vertruyen, R. Cloots, and R. Funahashi, *Mater. Res. Bull.* 43, 394 (2008). doi:10.1016/j.materresbull.2007.02.043.
14. M. Hervieu, A. Maignan, C. Michel, V. Hardy, N. Creon, and B. Raveau, *Phys. Rev. B* 67, 045112 (2003). doi:10.1103/PhysRevB.67.045112.
15. A. Maignan, D. Pelloquin, S. Hebert, Y. Klein, and M. Hervieu, *Bol. Soc. Esp. Ceram. V* 45, 122 (2006).
16. J. Liu, H.S. Yang, Y.S. Chai, L. Zhu, H. Qu, C.H. Sun, H.X. Gao, X.D. Chen, K.Q. Ruan, and L.Z. Cao, *Phys. Lett. A* 356, 85 (2006). doi:10.1016/j.physleta.2006.03.016.
17. M. Karppinen, H. Fjellvåg, T. Konno, Y. Morita, T. Motohashi, and H. Yamauchi, *Chem. Mater.* 16, 2790 (2004). doi:10.1021/cm049493n.